34P.

NOTICE

The invention disclosed in this document resulted from
research in aeronautical and space activities performed under
programs of the National Aeronautics and Space Administration.
The invention is owned by NASA and is, therefore, available for
licensing in accordance with the NASA Patent Licensing
Regulation (14 Code of Federal Regulations 1245.2).

To encourage commercial utilization of NASA-owned inventions,
it is NASA policy to grant licenses to commercial concerns.
Although NASA encourages nonexclusive licensing to promote
competition and achieve the widest possible utilization, NASA
will consider the granting of a limited exclusive license,
pursuant to the NASA Patent Licensing Regulations, when such a
license will provide the necessary incentive to the licensee to
achieve early practical application of the invention.

Address inquiries and all applications for license for this
invention to NASA Resident Office-JPL, NASA Patent Counsel,
Mail Code 180-801, 4800 Oak Grove Dr., Pasadena, CA 91103.
Approved NASA forms for application for nonexclusive or
exclusive license are available from the above address.

FIG.1(a)

FIG.1(b)

Electron Injection   Electron Mirroring

ION CYCLE: Ion Repelling   Ion Extraction

FIG.2

ELECTRON TRAJECTORIES

Radial Distance

Axial Distance
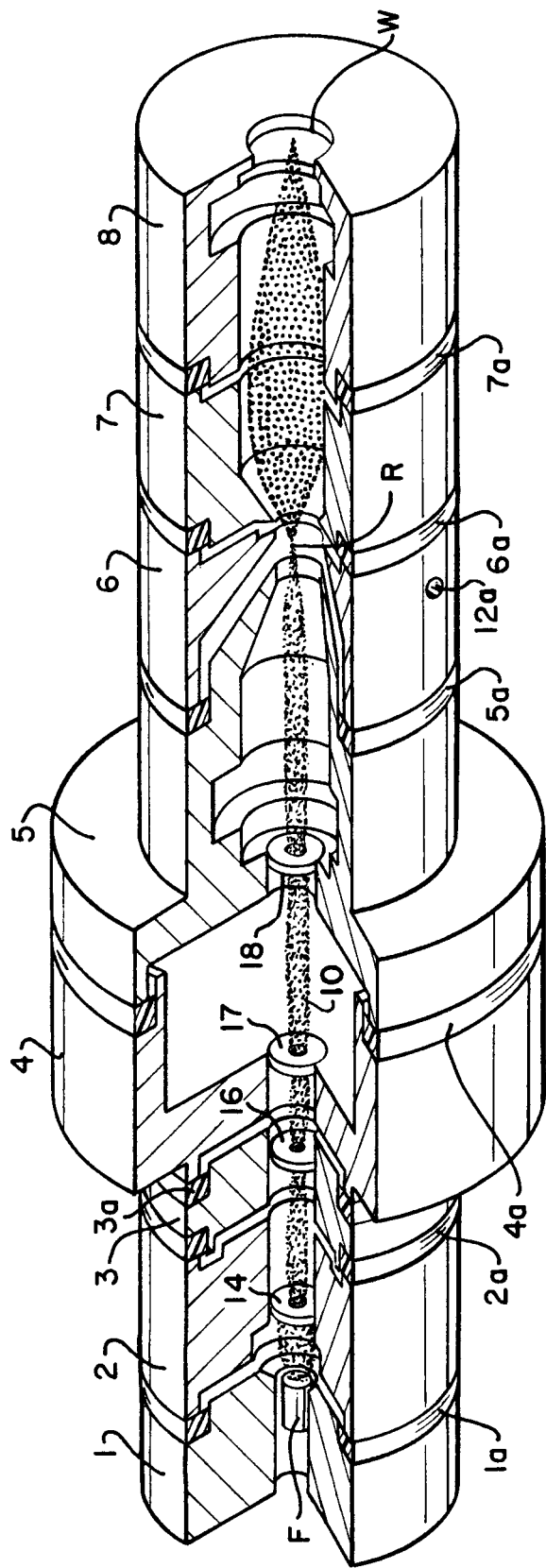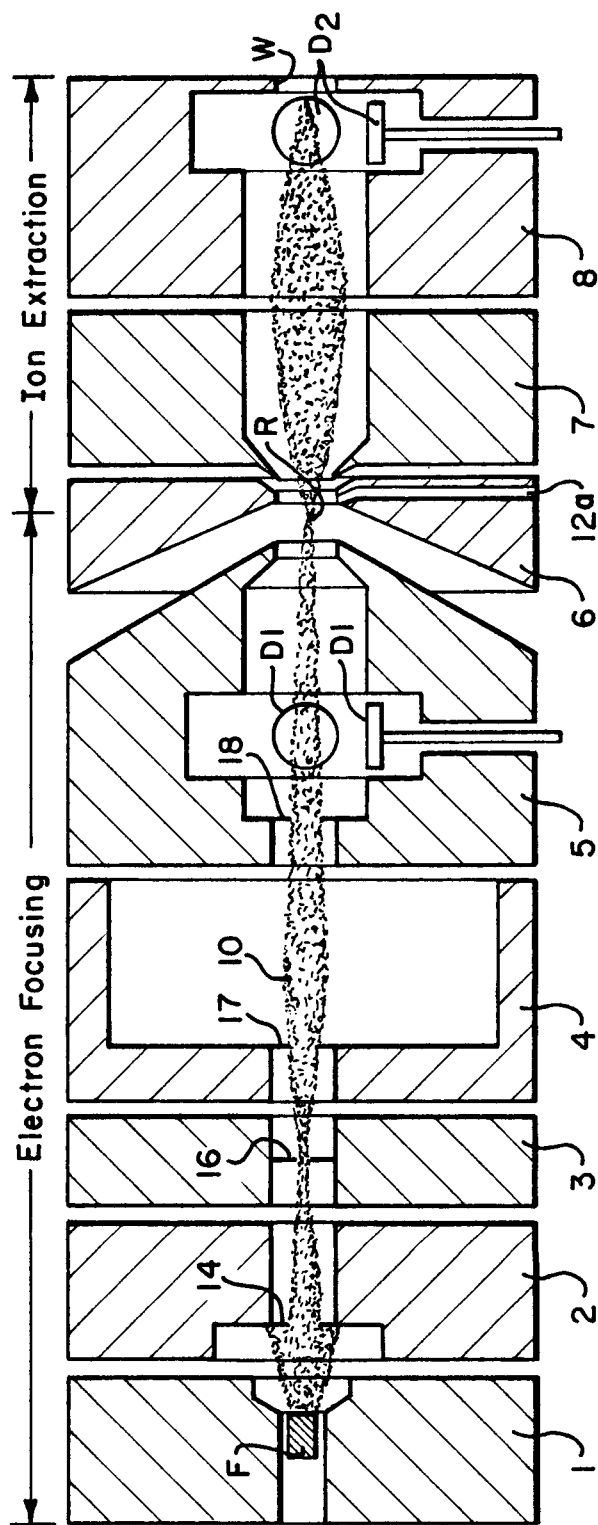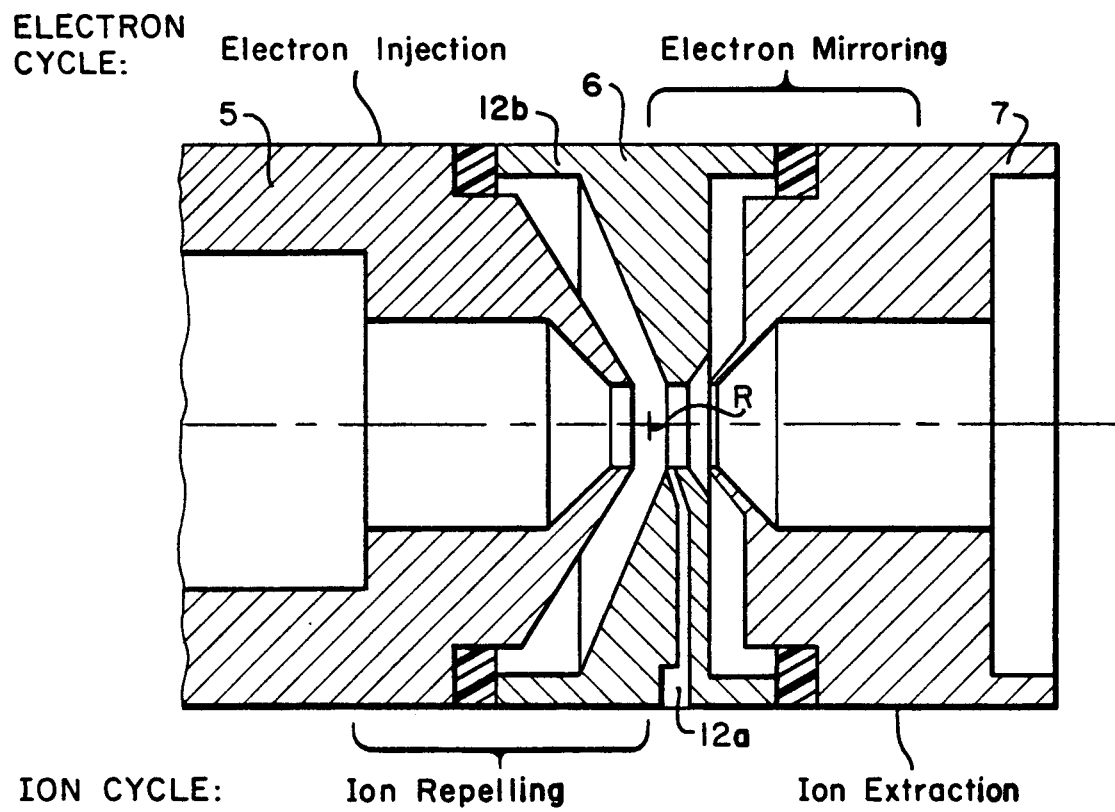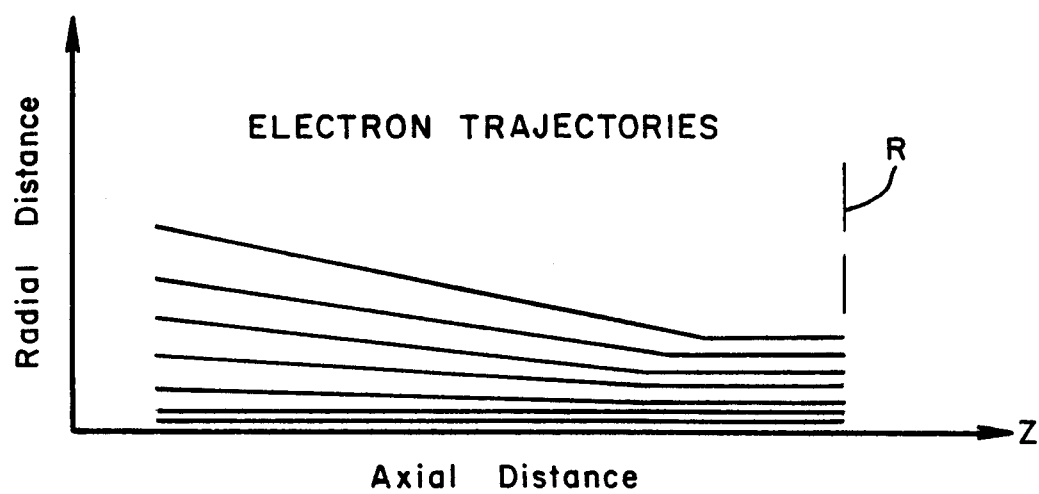
FIG. 3(b)
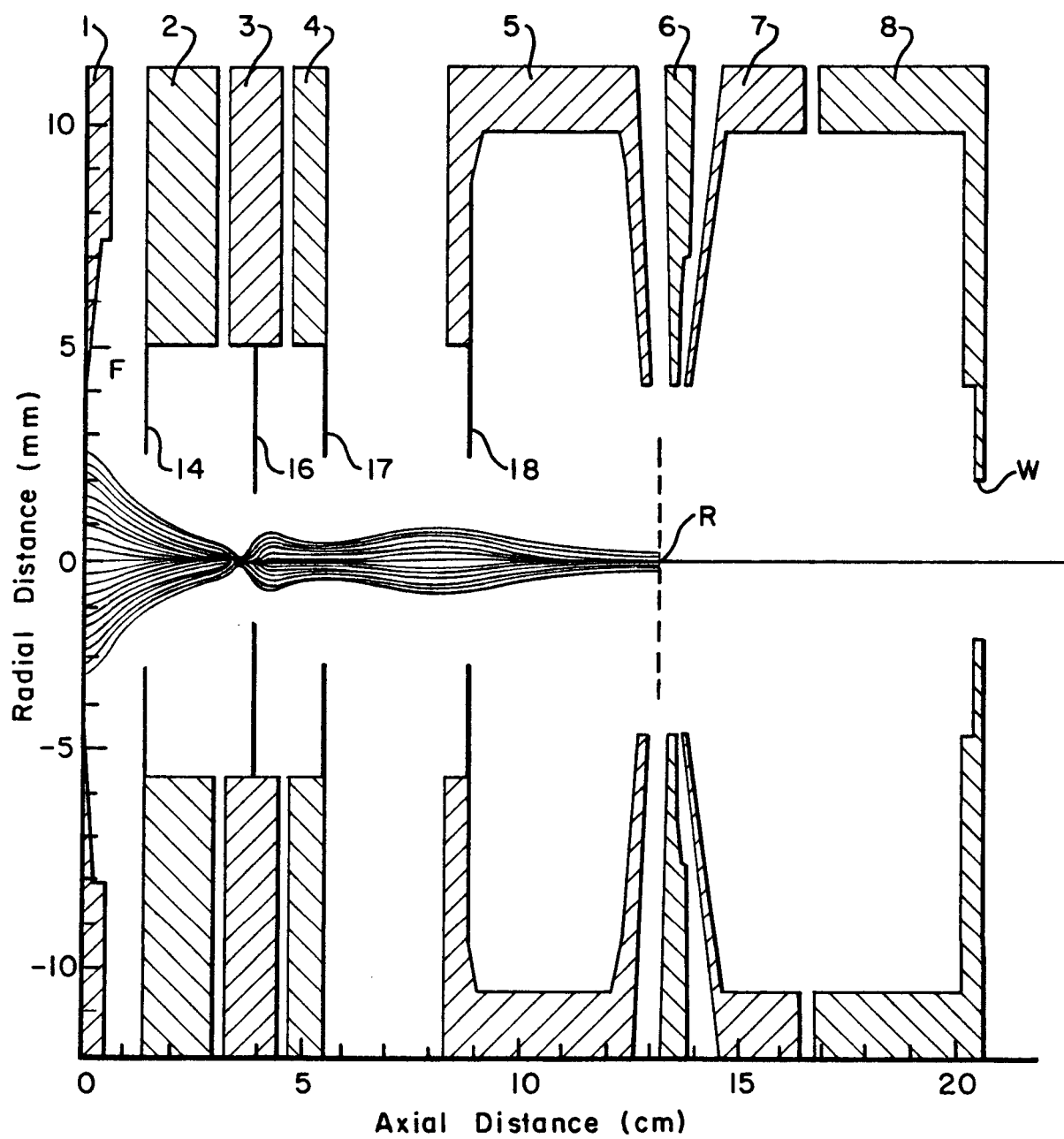
FIG. 3(a)

FIG. 3(c)
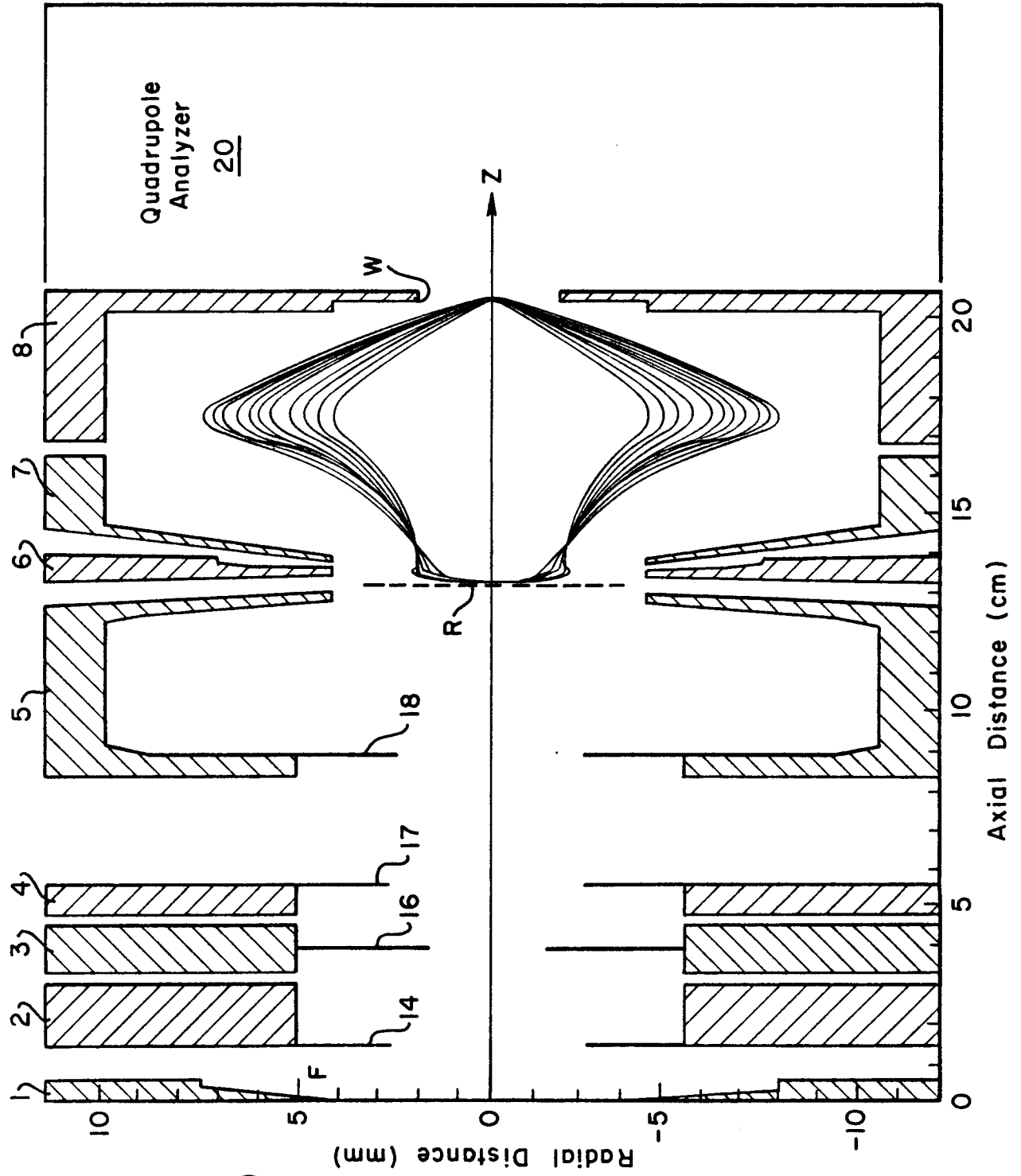
REVERSAL ELECTRON ATTACHMENT
IONIZER FOR DETECTION OF TRACE SPECIES

Inventors: Mark T. Bernius
             Ara Chutjian
Contractor: Jet Propulsion Laboratory

NASA Case No. NPO 17596-1-CU
April 27, 1989

AWARDS ABSTRACT

The invention relates to a high-sensitivity ion producing apparatus for trace species detection, and more particularly to a combined in-line electron beam generator, trace species ionizer, and an ion extractor utilizing an electrostatic mirror field to form a planar wall of electrons having as low as zero kinetic energy for electron attachment to molecules of an analytic gas.

FIGs. 1a and 1b illustrate the invention comprised of electrodes 1 through 8 capable of focusing a beam of electrons to a reversal region R and executing a reversal of the electrons, such that the electrons possess zero kinetic energy at the point of reversal and then extracting ions produced. By adjustment of the axial position for the reversal region R relative to the point where a sample gas is introduced through a port 12a, the invention may be used to produce both negative and positive ions. For negative ions, the reversal region R is positioned where the sample gas is introduced for low energy electron-molecule attachment with high efficiency using the electrodes 5, 6 and 7, as illustrated in FIG. 2, to produce electron trajectories as shown in FIG. 3(b). Ions produced are extracted and directed to a mass analyzer by switching the potentials applied to electrodes 5, 6 and 7 from an electron cycle to an ion cycle, as shown in FIG. 2, where they may be detected and identified. The generation and detection of positive ions is accomplished in a similar fashion with minimal adjustment to potentials applied to shift the reversal region to the right slightly past the point where the sample gas is introduced. FIGs. 3(a) and 3(b) illustrate the electron and ion trajectories for the electron and ion cycles, respectively, as plotted from a computer model to a larger scale of radial distance for clarity. FIG. 4(a) illustrates typical ion arrival-detection characteristics as seen on an oscilloscope for Cl^- production from CCl_4 during an ion cycle and an electron cycle (square wave train) with ions arriving for detection shortly after the ion cycle is turned on, and FIG. 4(b) shows in greater detail the ions arriving shortly after the ion cycle is turned on in the graph of FIG. 4(a) where the ion burst arrives at the detector approximately 15 µs after ion extraction voltage is applied, which corresponds to the chlorine ion's time-of-flight from the ion extractor through the quadrupole and to the detector. FIG. 5(a) illustrates Pierce extraction geometry showing the inclined V and V' surfaces used to extract a linear flow of electrons from the planar electron emitter in rectangular coordinates, and FIG. 5(b) illustrates time-reversed electron flow in an analogous Pierce geometry (in cylindrical-polar coordinates) to achieve electron reversal at a point R of an imaginary cathode. FIGs. 6(a) and (b) illustrate the electrode pulsing sequence for extraction of negative and positive ions, respectively. FIGs. 7(a) through (f) illustrate mass spectra of attachment and dissociative attachment in CCl_4, SF_6, $CHCl_3$, $1,1,2-C_2Cl_3F_3$ and $c-C_6F_{10}$ achieved with the present invention. The resonances in FIGs. (c) and (d) are at nonzero electron energy while those in FIGs. (a), (b), (e) and (f) correspond to virtual states at zero energy. FIG. 8 is a graph of sensitivity evaluation data of the present invention using the method of standard additions analysis for various concentrations of CCl_4 in N_2.

The novelty of the invention resides in the in-line arrangement of electrodes with time sharing of electrodes 5, 6 and 7 as shown in FIG. 2, and the production of electron trajectories as shown in FIG. 3(a) and 3(b) with electrons approaching the reversal plane along parallel paths with no lateral motion at the point of reversal for each electron.
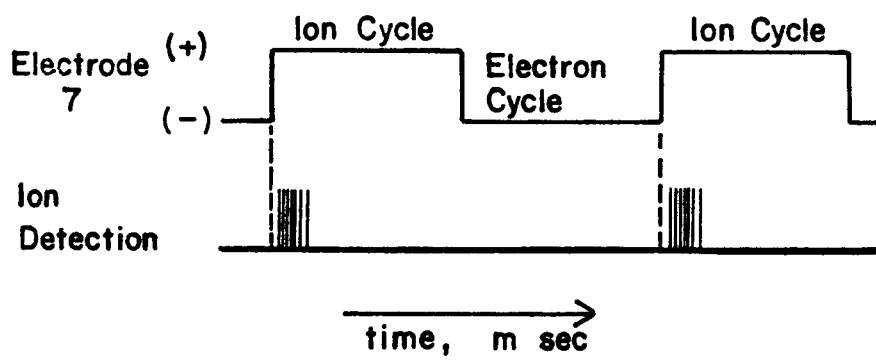
FIG.4(a)
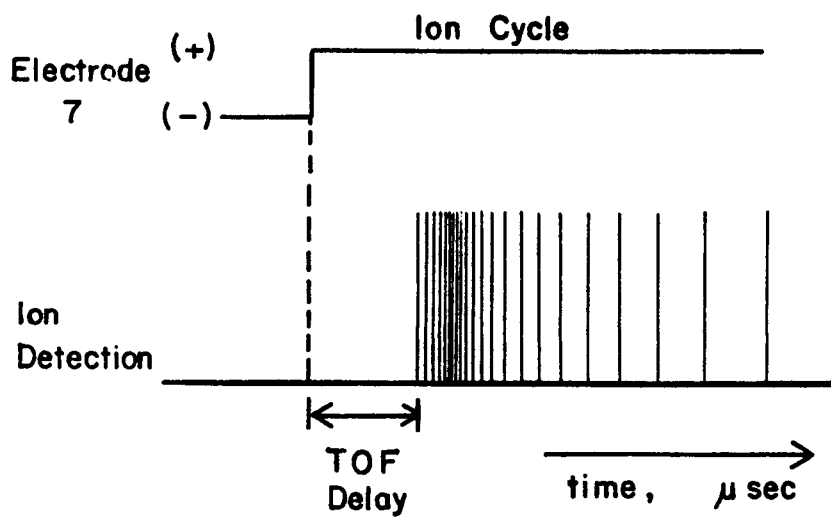
FIG.4(b)
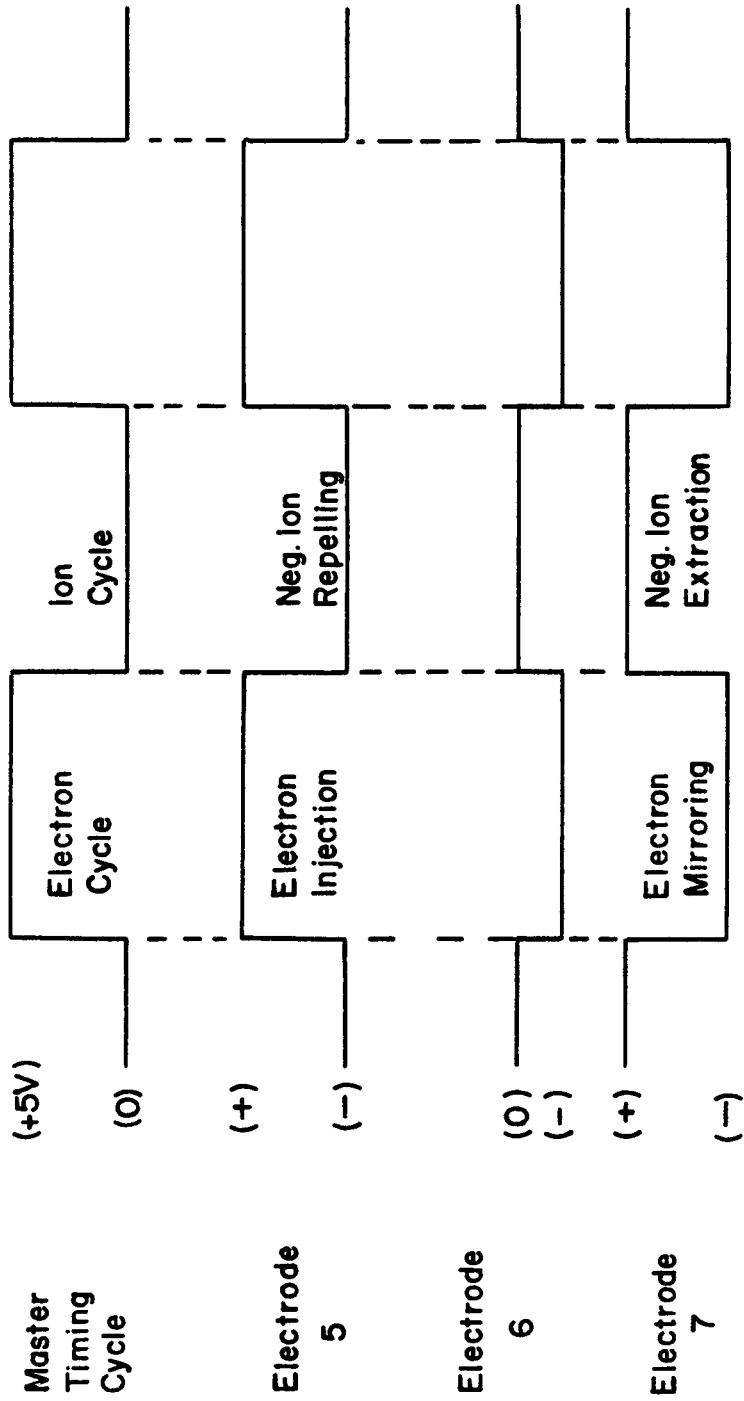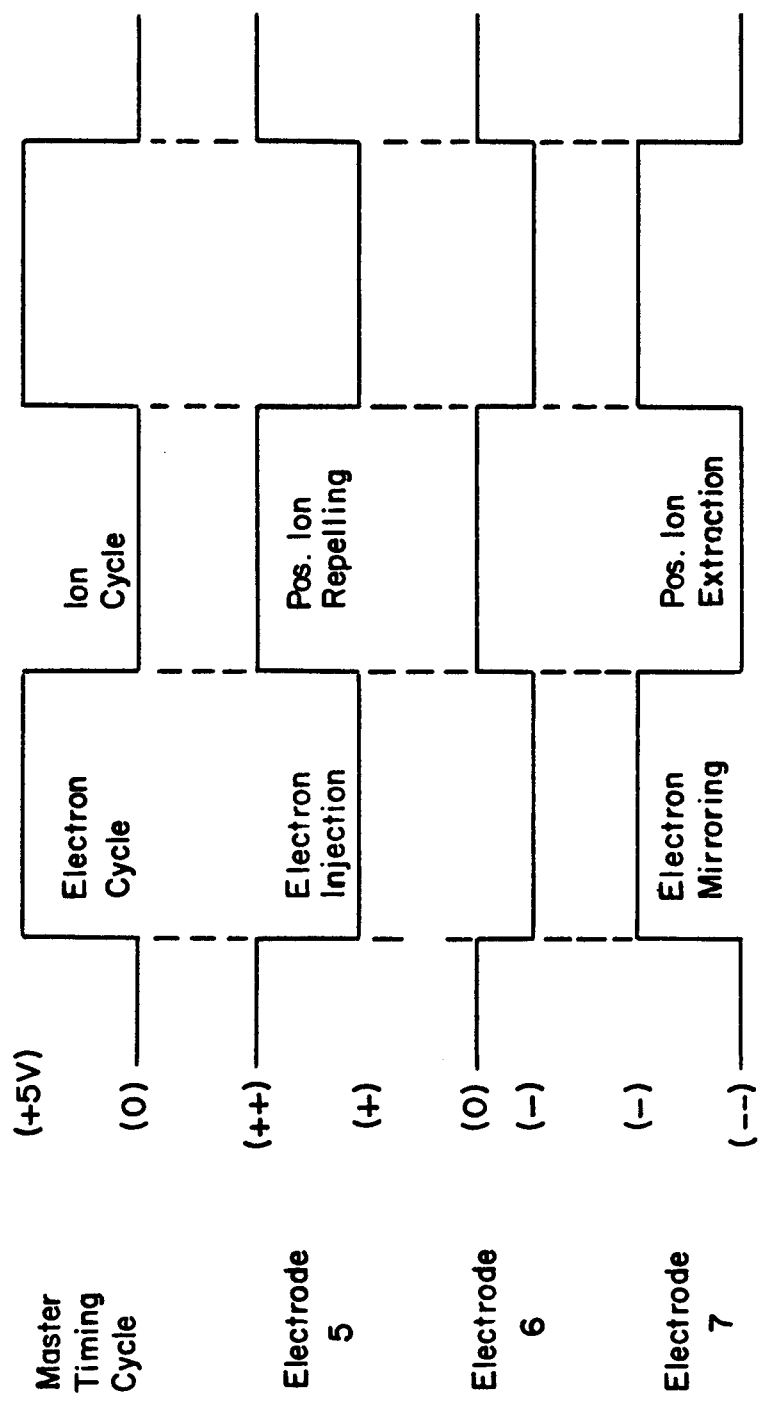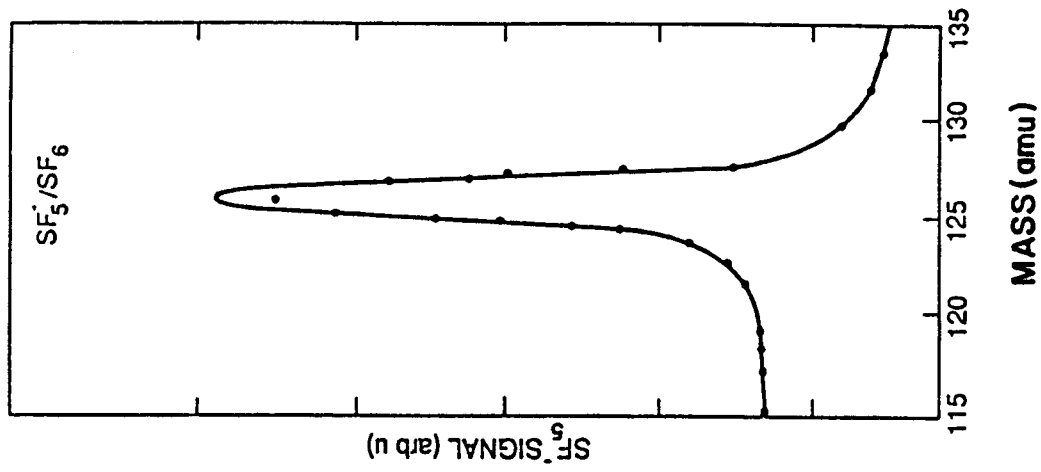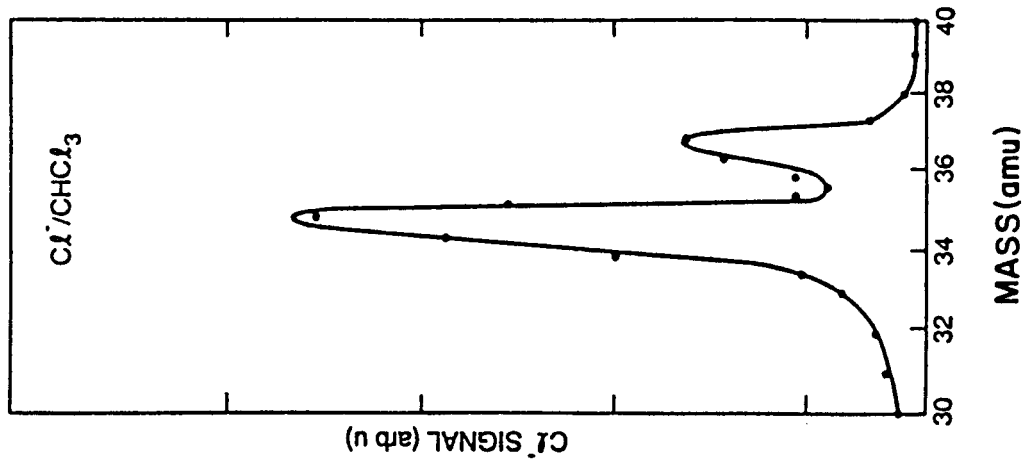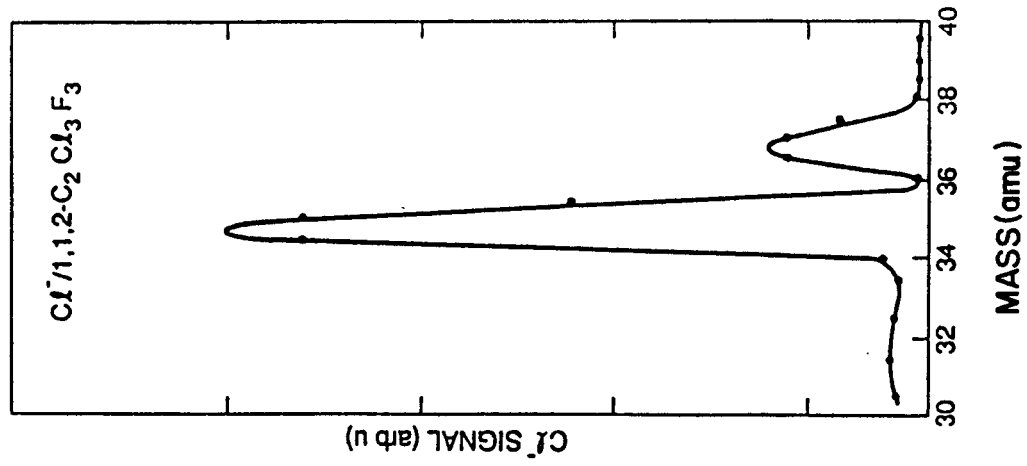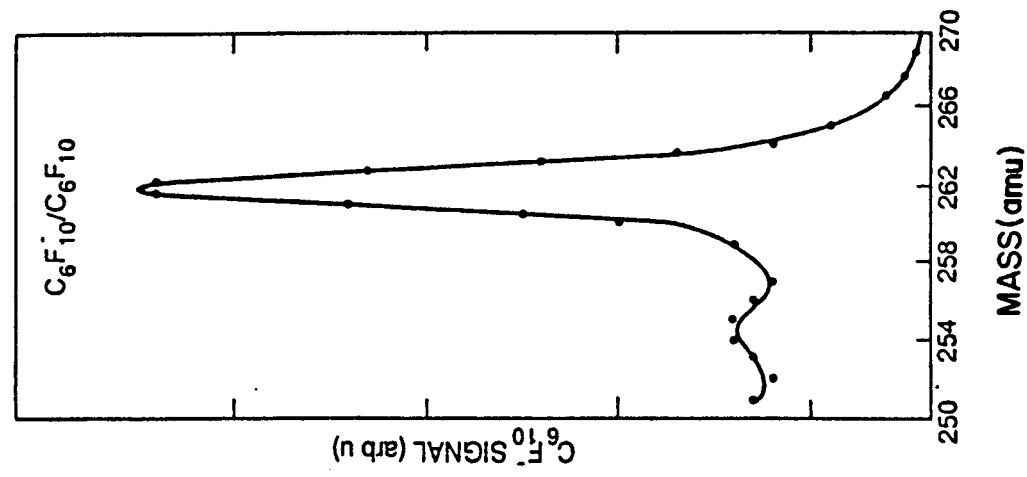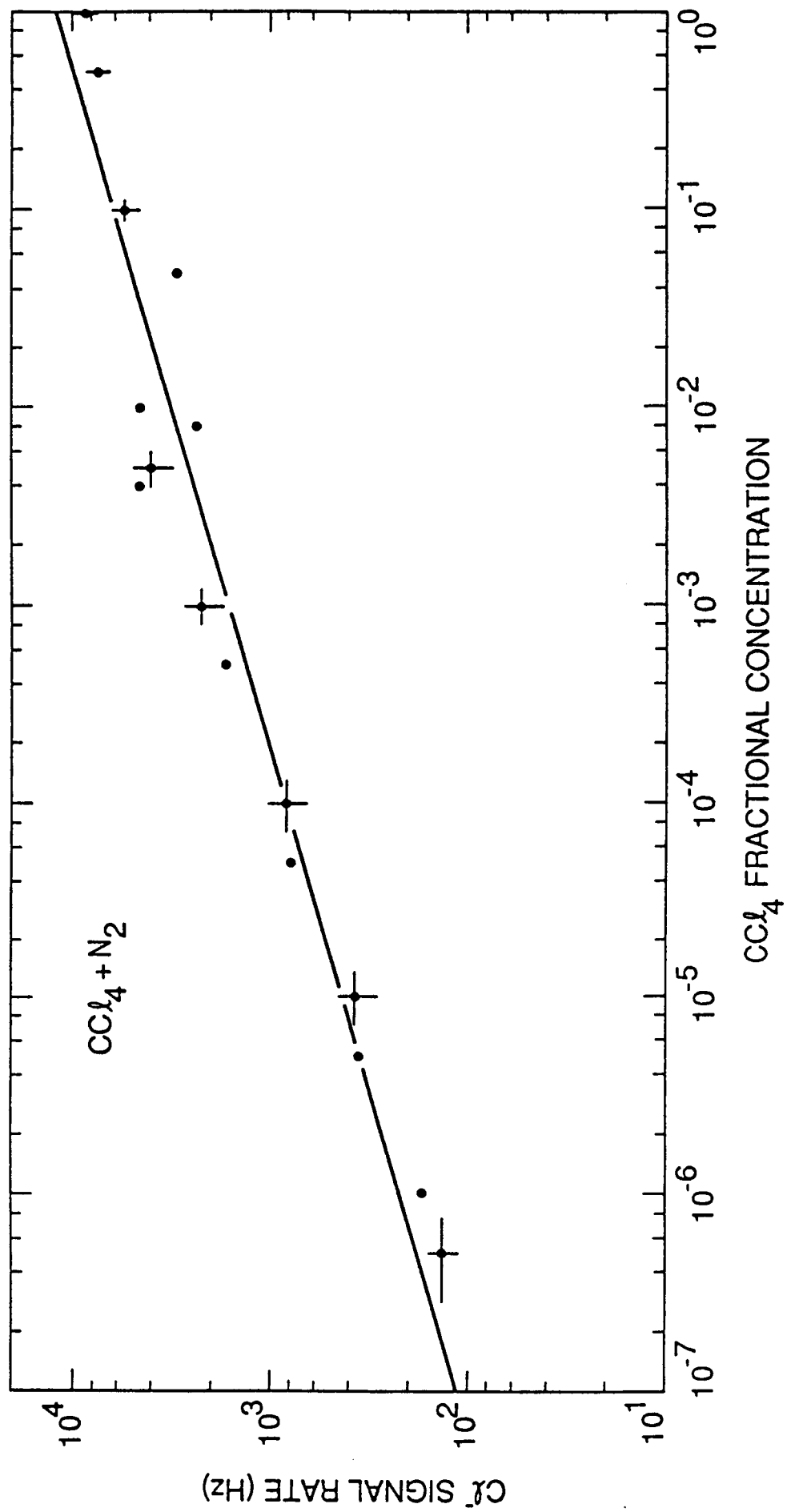
V = 0

V = V'
PROJECTOR
ELECTRODE

Z

e⁻

$\theta = \dfrac{3\pi}{8}$

REVERSAL PLANE

R

r

FIG.5(b)

V = V'
ANODE

V = 0

X

e⁻

$\theta = \dfrac{3\pi}{8}$

0

Y

CATHODE

FIG.5(a)

Master
Timing
Cycle

(+5V)

(0)

Electron
Cycle

Ion
Cycle

Electrode
5

(+)

(−)

Electron
Injection

Neg. Ion
Repelling

Electrode
6

(0)
(−)

Electrode
7

(+)

(−)

Electron
Mirroring

Neg. Ion
Extraction

FIG. 6(a)

FIG.6(b)

FIG.7(a)

FIG.7(b)

FIG.7(c)

FIG.7(f)

C₆F₁₀⁺/C₆F₁₀ — $C_6F_{10}^{\cdot}/C_6F_{10}$

$C_6F_{10}^{-}$ SIGNAL (arb u)

MASS(amu)

FIG.7(e)

$Cl^-/1,1,2\text{-}C_2Cl_3F_3$

Cl^- SIGNAL (arb u)

MASS(amu)

FIG.7(d)

$Cl^-/CHCl_3$

Cl^- SIGNAL (arb u)

MASS(amu)

CCℓ₄ + N₂

CCℓ₄ FRACTIONAL CONCENTRATION

Cℓ SIGNAL RATE (Hz)

FIG. 8

Serial No. 361,531

Filing Date 6/5/89

PATENT

(City) (State) (Zip)

REVERSAL ELECTRON ATTACHMENT
IONIZER FOR DETECTION OF TRACE SPECIES

Origin of the Invention

5   The invention described herein was made in the perform-
ance of work under a NASA contract, and is subject to the
provisions of Public Law 96-517 (35 USC 202) in which the
Contractor has elected not to retain title.

10   ### Technical Field

The invention relates to a high-sensitivity ion produc-
ing apparatus for trace species detection and more particu-
larly to a combined in-line electron beam generator, trace
species ionizer, and an ion extractor utilizing an electro-
15   static mirror field to form a planar wall of electrons having
as low as zero kinetic energy for electron attachment to
molecules of an analytic gas.

Background Art

20   There exists a large number of molecules capable of
attaching a zero or near-zero energy electron to form a nega-
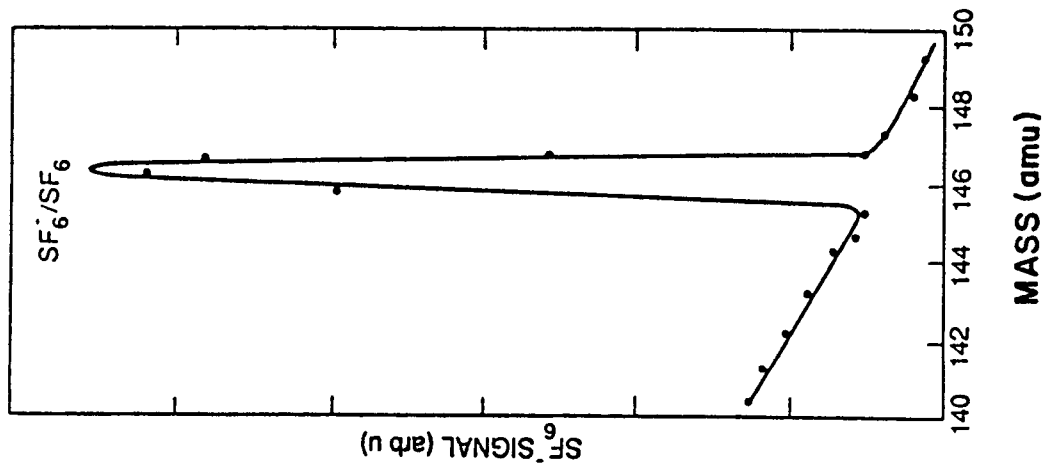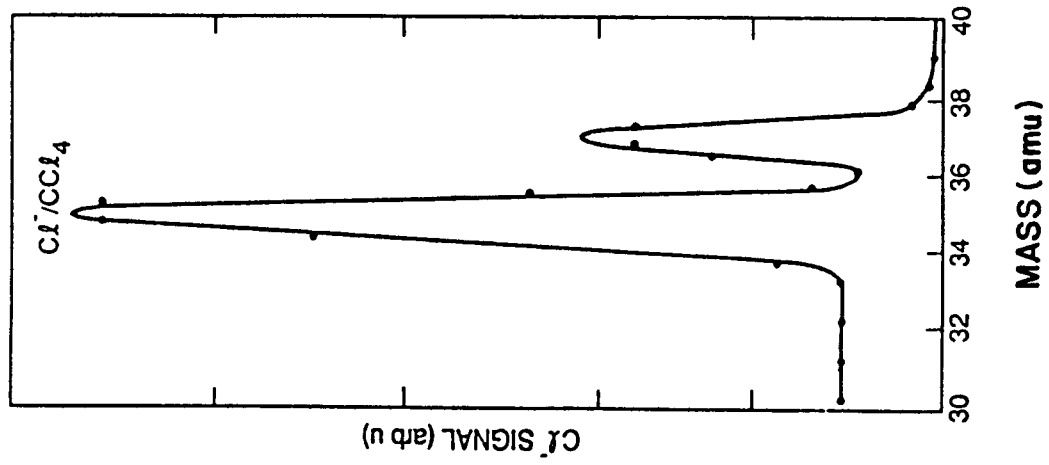tive ion. This ion may be the parent negative ion, or a
fragment atomic or molecular ion formed via dissociative
attachment. Energetically, the curve-crossing between the
25   lowest neutral and negative ion states is made possible by the
fact that the electron affinity of some atomic (e.g., F, Cl,
Br, I) or molecular (e.g., CN) component is comparable to the
dissociation energy of the neutral target. From symmetry
considerations, the neutral-ion transition at zero electron
30   energy often involves a transition between states of the
symmetric irreducible representation, except possibly the
halogen molecules. As such, the energy and symmetry require-
ment fulfill the s-wave threshold law in which the attachment
cross section is $\sigma_A(E) \approx E^{\ell - 1/2}$, where ℓ is the angular momentum

component of the captured electron, and E the electron energy. For $\ell=0$(s-wave) attachment, A. Chutjian and S.H. Alajajian, Phys. Rev. A **31**, 2885 (1985), were the first to demonstrate for the molecular case that the attachment process diverges as

5      $\sigma_A(E) \approx E^{-1/2}$. This s-wave attachment divergence had been studied earlier in nuclear physics by others in thermal neutron capture by light nuclei. See E.P. Wigner, Phys. Rev. **73**, 1002 (1948); H.A. Bethe, Rev. Mod. Phys. **9** 69 (1937).

       In an effort to utilize the divergent, zero-energy

10   cross sections in SF_6 and the chlorohalocarbon compounds, a technique was disclosed by A. Chutjian, et al., U.S. Patent No. 4,649,278, to focus an electron beam into an electrostatic mirror, where at the point of "reversal" the longitudinal electron energy was theoretically reduced to zero. In prac-

15   tice, only a fraction of electrons actually reach absolute zero energy at the point of reversal because of the lateral (transverse) velocity acquired in the electron gun. The beam of reversed electrons resembles a water fountain having a spray of finite vertical velocity and limited diameter up to

20   the reversal region and a return spray of greater and spreading diameter. This spreading of the return flow of electrons results from a lack of shaped electrodes for electrostatic confinement in the reversal region where the electron beam achieves near-zero energies. Thus, after introduction of a

25   beam of thermal-attaching molecules, negative ions were extracted from the collision center via the s-wave, dissociative attachment state, but no efforts were made in this earlier development to optimize electron current, reversal geometry, and extraction efficiency; nor were provisions made to mini-

30   mize the transverse energy spread of the electrons at the reversal point.

       In order to use this reversal electron attachment technique for ionization and ion-extraction of trace species at very low electron energies, the problem is to generate a

35   large density of thermal electrons in the reversal region

where attachment to molecules of extremely low concentration is to take place.

Statement of the Invention

5   An in-line reversal electron, high-current ionizer-detector capable of focusing a beam of electrons to a reversal region of zero kinetic energy to produce negative ions through single collision electron attachment. By suitable adjustment of polarities, it can also produce positive ions

10   through collisional ionization of the trace species by electrons of higher energy. Electron attachment to a molecular target in the reversal region produces parent or fragment negative ions through a zero-energy (s-wave) virtual state. The ions are pulsed out of the collision region to a quadru-

15   pole mass analyzer in line with the electron beam generator.

A planar wall of zero-energy electrons is created by focusing the electrons into parallel paths through shaped electrostatic fields to a plane where the electostatic field effects a reversal of the electron trajectories while con-

20   tinuing to confine the electrons to the same parallel paths in the region of reversal. This provides a high density of thermal electrons of energies that approach and reach zero energy in the reversal region, with no transverse energy. The analytic gas is continuously introduced at the reversal region

25   for ionization. Extracted ions are focused into a window of an in-line mass spectrometer operated in the negative-ion mode.

Brief Description of the Drawings

30   FIG. 1(a) is an isometric view of the electron gun, electron reversal, and ion extraction lens systems of the present invention partially sectioned, and FIG. 1(b) is a schematic cross section diagram of the structure in FIG. 1(a).

FIG. 2 illustrates details of the shaped electrodes

35   shared for electron reversal and ion extraction.

FIG. 3(a) is a graph of electron trajectories calcu-
lated up to a reversal region R during the "electron on" half
cycle, FIG. 3(b) is a graph of the reversal region showing the
time-reversed Pierce-element behavior, resulting in a vertical
5   "wall" of electrons at R with zero transverse and longitudinal
energy, and FIG. 3(c) is a graph of ion trajectories calcu-
lated up to an entrance window W of a quadrupole analyzer
during the "ion on" half cycle.

FIG. 4(a) illustrates typical ion arrival-detection
10 characteristics as seen on an oscilloscope for Cl^- production
from CCl_4 during an ion cycle and an electron cycle (square
wave train) with ions arriving for detection shortly after the
ion cycle is turned on, and FIG. 4(b) shows in greater detail
the ions arriving shortly after the ion cycle is turned on in
15 the graph of FIG. 4(a) where the ion burst arrives at the
detector approximately 15 μs after ion extraction voltage is
applied, which corresponds to the chlorine ion's time-of-
flight from the ion extractor through the quadrupole and to
the detector.

20   FIG. 5(a) illustrates Pierce extraction geometry show-
ing the inclined V and V' surfaces used to extract a linear
flow of electrons from the planar electron emitter in rectan-
gular coordinates, and FIG. 5(b) illustrates time-reversed
electron flow in an analogous Pierce geometry (in cylindri-
25 cal-polar coordinates) to achieve electron reversal at a point
R of an imaginary cathode.

FIGs. 6(a) and (b) illustrate the electrode pulsing
sequence for extraction of negative and positive ions, respec-
tively.

30   FIGs. 7(a) through (f) illustrate mass spectra of
attachment and dissociative attachment in CCl_4, SF_6, $CHCl_3$,
$1,1,2-C_2Cl_3F_3$ and $c-C_6F_{10}$ achieved with the present invention.
The resonances in FIGs. (c) and (d) are at nonzero electron
energy while those in FIGs. (a), (b), (e) and (f) correspond
35 to virtual states at zero energy.

FIG. 8 is a graph of sensitivity evaluation data of the present invention using the method of standard additions analysis for various concentrations of CCl_4 in N_2.

5   Theory of Resonances

The formal theory of resonances, virtual states, bound states, and their behavior at threshold has been given within several frameworks and applied in specific instances to diatomic and polyatomic scattering. In the following paragraphs,

10 a heuristic picture of the attachment process is presented, concentrating somewhat more on a physical picture rather than on the theoretical formalism.

For electrons e(E) of energy E and a target molecule AB in vibrational state v, the process of electron attachment

15

$$e(E)+AB(v=0) \rightarrow AB^-(v>0) \qquad (1a)$$
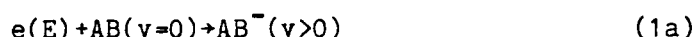
and dissociative attachment (DA)

20

$$e(E)+AB(v=0) \rightarrow A+B^- \qquad (1b)$$

constitute major reaction channels that influence the behavior of the upper atmosphere, lasers, electrical discharges, lamps, gaseous insulators, circuit breakers and high-power diffuse-

25 discharge switches. They are also the principal reaction channels upon which the electron-capture detector (ECD), used in chromotographic studies, is based: namely, that one influences the current in a detection circuit by converting a mobile electron into a sluggish negative ion via Equations

30 (1a) and (1b).

The model considered here is one in which a new bound, virtual negative-ion state is born at threshold, i.e., with a large s-wave component. See J. P. Gauyacq and A. Herzenberg, J. Phys. B 17, 1155 (1984). The mechanism of electron capture

35 is a nonadiabatic coupling of the neutral target and a nega-

tive-ion state formed by the "loosely bound" electron. The
virtual state is associated with a pole on the negative k-axis
in the complex k plane. The effect of this pole, lying
slightly below the origin, is to cause at low electron ener-
gies enhancement of the amplitude of the electron wavefunction
at the target relative to the incident wave. No angular-
momentum trapping and time-delay is involved, such as in a
shape or Feshbach resonance at higher electron energies. See,
for example, A. Herzenberg and B.C. Saha, J. Phys. B **16**, 591
(1983). The enhancement of the electron's wavefunction at the
molecular boundary is brought about by constructive interfer-
ence between the incoming s-wave of the form (sin kr)/kr, and
the outgoing wave of the form (cos kr)/kr. In the limit of
small energy kr≪1, the ratio of amplitudes becomes

$$\left(\frac{\cos kr}{kr}\right) \bigg/ \left(\frac{\sin kr}{kr}\right) \ = \ \approx (kr)^{-1} \approx \ll \frac{\lambdabar}{r} \tag{2}$$

where $\lambdabar$ is the reduced deBroglie wavelength, and r is the
electron-molecular center distance. For $r \approx 4a_o$ and k=0.027au
(0.01 eV), this enhancement is a factor of 9.2 in amplitude,
or 85 in intensity.

Following the treatment of Gauyacq and Herzenberg cited
above, one may express the attachment of DA cross section
$\sigma_a(E)$ as

$$\sigma_A(E) \ = \ \frac{4\pi^2}{\sqrt{2}} \ |A_{v0}|^2 E^{-1/2} \tag{3}$$

where E is the electron energy in au, and A_{v0} is the amplitude
of the wavefunction $\Psi(r,R)$ in the time-reversed calculation
for an ion-atom collision.

$$\Psi(r,R) \ = \ \sum_v A_v \chi_v(R) \ \frac{\exp(ik_v r)}{r} \tag{4}$$

Here, r is the electron's distance from the AB⁻ center of
mass, R the A⁻-B nuclear distance, k_v the electron momentum as
it collides with the vibrational level v in AB⁻, and $\chi_v(R)$ is
the vibrational wavefunction of level v as a function of
5   internuclear distance. Equation (4) describes a spherical
outgoing electron wave which was detached in the A⁻-B colli-
sion, leaving AB(v) in the vth vibrational level. The colli-
sion corresponds to the time-reversed process AB(v)+e→AB⁻(v')
so that the scattering cross sections are related by detailed
10   balance. The important feature of Equation (3) is that, in
the limit of E→0, the outgoing amplitudes A_v become slowly
varying with respect to $E^{-1/2}$ so that the attachment cross
section exhibits the $E^{-1/2}$ divergence.

The negative ion thus formed can have several fates. If
15   a dissociative channel is energetically open, the ion will
fragment in the course of a single vibration. An example of
this dissociative attachment [Equation (1b)] is the breakup
$e+CCl_4 \rightarrow CCl_3 + Cl^-$. If the negative ion is stable with respect
to dissociation, then the total electron + vibrational energy
20   will be distributed throughout the molecular ion normal modes:
its vibrational phase space is dramatically increased to the
point where one has a quasicontinuum of translation-like
energy levels. Such a state can exist for times on the order
of tens of microseconds, after which it may (a) autoionize to
25   the neutral target state, (b) be stabilized by collision with
another molecule, or (c) become detected in an experiment
prior to autoionization.

The present invention efficiently generates molecular
ions via negative or positive-ion formation at electron ener-
30   gies from zero electron volts to high energies (50 eV or
greater). By optimizing instrumental factors, these molecules
can be detected at the parts-per-billion level and better.

DETAILED DESCRIPTION OF THE INVENTION

(a) Overview

Referring to a schematic diagram of the apparatus shown in **FIGs. 1(a)** and **1(b)** for effecting electron capture (nega-
5   tive-ion formation) to molecules at low electron energies, a high current-density electron beam **10** is brought to a well-controlled reversal region **R** such that at the reversal point, the lateral and longitudinal components of the electron's kinetic energy are zero. A sample gas of interest is intro-
10   duced into the reversal region **R** through a port **12a**, and owing to the extremely large attachment cross section of this inter-action energy, an extremely efficient means for production of negative parent molecular ions is provided.

High-speed pulsed electronics switch the apparatus of
15   **FIG. 1** from molecular negative-ion generation (employing electron optics described below) to the collection and focus-ing of these ions (employing in-line ion extraction optics described below) to a suitable means of performing mass analy-sis and detection, such as a quadrupole analyzer shown in **FIG.**
20   **3(c)**. The shaped electrodes (electron optical components) **1-8** are individually controlled, with the electrode **6** shared for electron injection and ion repulsion, as shown in **FIG. 2**, during both the electron injection-reversal cycle, and the ion extraction cycle, providing an efficient instrument for analy-
25   sis of trace species. In actual practice, the electron beam is pulsed on for about 50 μs and then off. After about 2 μs, in-line ion extraction electrodes are pulsed on. Ion collec-tion efficiency is on the order of 100%, and estimated detec-tion limits can be on the order of 100 ions per cubic
30   centimeter of sample gas.

In accordance with a further feature of the invention, it is possible to not only bring the electrons to a zero-ener-gy (reversal) focus in the interaction region **R** but to a higher energy focus as well in order to either (a) generate
35   negative ions through attachment processes occurring at near

zero electron energies, or (b) effect positive ionization of the trace species at higher electron energies. The ion extraction in both cases is carried out with the same apparatus, except that extraction potentials in the case of positive ion

5   extraction are reversed.

Referring to **FIG. 1(a)** and **1(b)** in more detail, electrons are generated at an indirectly heated cathode F having a planar face, and focused by shaped annular electrodes (lens elements) **1-6** to the reversal region **R.** Insulating spacers

10 **1a** through **5a** shown in **FIG. 1(a)** isolate the electrodes **1-6** so that they may be operated at independent potentials in providing an electrode beam with reversal at the region **R.** The gas sample of target trace species is continuously introduced at this point through the port **12a** and vented through a larger

15 port **12b,** and either negative ions are formed by attachment of electrons in the energy range 0-20 eV, or positive ions are formed by bombardment with electrons having energy of about 40 eV.

The electrons are injected by impressing suitable

20 negative and positive voltages on respective annular electrodes **5, 6** and **7,** as shown in **FIGs. 6(a)** and **(b)** for negative and positive ions, respectively. The voltages are then switched for ion extraction and within 2 μsec the negative ions are extracted through a window **W.** Insulating spacers **6a**

25 and **7a** (optional) shown in **FIG. 1(b)** isolate the electrodes **6, 7** and **8** so that they may be operated at independent potentials while producing the electrons beam and then while extracting ions from the region **R.** This sharing of electrodes for electron injection and reversal and for ion extraction is illus-

30 trated in **FIG. 2.** The duty cycle of the voltage switching can be 50%, with 100% extraction efficiency of the ions during each ion cycle. Orthogonal deflectors D_1 shown in **FIG. 1(b)** may be used to provide small electrostatic deflection forces on the electron beam for fine tuning of the beam position at

35 the center (axis) of the region **R.**

The negative ions are focused at the plane of the exit window **W** by electrode **8** biased at a potential, negative for negative ions and positive for positive ions, to confine the ions within a spot size, and with a divergence

5   angle and final energy appropriate to either a quadrupole mass analyzer or time-of-flight analyzer. Orthogonal deflectors D_2 shown in **FIG. 1(b)** may be used to provide small electrostatic deflection forces on the ion beam for fine tuning of the beam position at the center (axis) of the exit window **W**. It should

10   be noted that a range of final electron energies can be provided at region **R** by establishing the reversal point between electrodes **5** and **6** relative to the electrode **7**.

Trajectories of electrons and ions were calculated using a full space-charge formulation, in which computer-

15   assisted design techniques are used to solve for the electrode geometry and potentials necessary to achieve the final trajectories plotted in **FIGs. 3(a), (b)** and **(c)**. The trajectories achieved are such that the reversed electron path exactly retraces itself as it returns toward the heated cathode **F**,

20   thus providing absolute zero-energy electrons in the reversal region **R**. This is accomplished by carefully choosing the shape of the electrodes **5-7**. If desired, an electron beam for nonzero bombardment may be provided to cross the sample gas target inlet positioned twice, once while proceeding left

25   to right and once while returning right to left. This nonzero energy electron beam affords a factor-of-two increase in effective electron beam density at the region **R**, and hence of ultimate ion detection sensitivity.

(b) Electron Cycle and Ion Cycle

30   Electrostatic field penetration or overlap, discussed by M.T. Bernius, K.F. Man and A. Chutjian, Rev. Sci. Instrum. **59**, 2418 (1988), has been incorporated in the present invention. The primary electron source is the heated cathode **F** which is planar and whose optical properties have been pre-

35   sented by Bernius, et al., in the paper just cited. The

electrons can be accelerated up to 600 volts and then extract-
ed through an aperture 14 in electode 2.   Electrode 3, in
which there would be significant field penetration except for
an aperture 16 placed therein, decelerates the beam and forces

5   a crossover in the neighborhood of its aperture. This crosso-
ver is imaged at the reversal region R by the shaped elec-
trodes (projector lens elements) 4-5 immediately following.
The final electrode 5 of the electron gun has the deflection
capability to center the beam on axis with fine tuning by

10   electrodes D_1.   A computed trajectory is shown in **FIG. 3(a)**.
Note that in the graphs of a computer model shown in **FIGs.
3(a), (b)** and **(c)** the scale of radial distance has been magni-
fied by a factor of ten for clarity relative to the axial
distances.

15   The beam is finally focused at a plane near the axial
midpoint of the shaped electrodes (electrostatic mirror ele-
ments) 5-6 which define the reversal region R.   These mirror
electrodes 5-6 are so shaped (designed) as to facilitate
formation of a collimated beam coming to zero longitudinal and

20   radial velocity at the reversal plane, as shown in **FIG. 3(b)**.
Therefore optical conditions to assure a proper match between
electron trajectories exiting the projector lens and those
necessary to achieve zero kinetic energy at the reversal plane
where the sample gas is injected are maintained by proper

25   choice of voltages on the electrodes 5 and 6.   The following
trajectories are then observed: paraxial rays of small angu-
lar divergence coming to a focus are "straightened out" to
parallel trajectories in the last few millimeters of beam
path, as depicted in **FIG. 3(b)**.   The electrons, now parallel

30   to the optical axis, come to a stop   with zero velocity in
both longitudinal and radial components of the particle's
velocity at the focal plane R, and reverse direction. In this
way, the optical principle of reciprocity is used to assure
complete reduction of the beam's energy, as will be more fully

35   discussed below.

The electron gun electrodes **1-5** and electron mirror electrodes **6-7** are designed to focus a 400 μA primary beam diameter to a 130 μm diameter in the reversal region. This are possible because the shaped electrodes compensate for

5   space charge. Beams of less current (and lower voltage) are easily accommodated with proper retuning of the operating electrode voltages. In actuality, the electron beam is not entirely of uniform electron energy, even though the electrode shapes and apertures along the path of the beam are intended

10   to favor electrons of uniform energy. An aperture placed at the major focal point of a chromatic lens will perform energy selection, favoring that energy band whose focal point corresponds to the aperture plane as a function of the aperture size. Likewise, an aperture stop placed at the Gaussian image

15   plane will also improve chromatic filtration when dealing with small cylindrically-symmetric object sources undergoing demagnification. See G.F. Rempfer and M.S. Mauck, J. Appl. Phys. **63,** 2187 (1988). Therefore, in practice, an ensemble of reversal conditions will exist in the neighborhood of the

20   calculated reversal plane **R.**

The terms "reversal plane" and "reversal region" are used to refer to substantially the same area of the electron beam path but with the more precise term "reversal plane R" as indicated in **FIG. 3(b)** when referring to the place of reversal

25   of the electrons, and the less precise term "reversal region R" when referring to the place of ionization of the sample gas. Note that the reversal plane **R** may be shifted to the right along the **Z** axis for nonzero energy ionization, i.e., for producing positive ions. For this reason, special provi-

30   sions are incorporated in the design of the ion-focusing electrodes **6-8** to select the position of the reversal plane, and to focus ions found there into the acceptance window **W** of the quadrupole mass analyzer **20** shown in **FIG.3(c)**. The shaped electrodes **6** and **7,** coupled with shaped electrodes **7** and **8,**

35   are quite selective. By matching operating voltages with

aperture size on the exit window **W** of electrode **8**, only those ions from a depth Δz of the reversal region **R** will be focused, mass analyzed and detected. For the present example of the invention, $\Delta z = 0.8$mm was used.

5   (c) Electron Focusing and Ion Extraction

The electron-focusing and ion-extraction operations shown in **FIGs. 3(a)** and **3(c)** are alternately switched on, as will now be described with reference to **FIG. 6(a)**. Electrons are focused and reversed at region **R** during one-half of a

10   square-wave switching cycle timing signal, then shut off by applying a large negative voltage on annular shaped electrode **5**. After a few microseconds into the second half of the cycle, the ions are extracted by a positive voltage on annular shaped electrodes while electrode **6** is held at zero volts.

15   Ion trajectories are shown in the computed simulation of **FIG. 3(c)**. Alternating between the electron cycle and the ion cycle is thus accomplished by switching voltages applied to shaped electrodes **5-7**. Those voltages are applied sufficiently fast so that the generated negative ions cannot drift from

20   their origin by more than about one-third the lens diameter during the time it takes to switch voltages.

During an electron cycle indicated in **FIG. 2**, the shaped electrode **5** is pulsed to a positive voltage (+40V) for focusing the electron trajectories as shown in **FIG. 3(b)**,

25   while the electrodes **6** and **7** are both held at a potential sufficiently negative (-10V) to produce electron reversal at the plane **R**. Electrodes **1, 2, 3** and **4** remain at their selected positive potentials with respect to the cathode voltage for shaping and focusing the electron beam **10**. Following an

30   electron cycle, an ion cycle indicated in **FIG. 2** is initiated by pulsing the electrode **7** to a high positive voltage (+850V) and the electrode **5** to a negative (-200V) potential while the electrode **6** is switched to zero volts, as shown in **FIG. 6(a)**. This repels negative ions away from the region **R** while the

35   positive electrode **7** extracts the ions. The shaped electrode **8**

remains at a positive potential for focusing the ion beam into the window **W**.

For producing positive ions by bombardment with elec-
trons, the reversal plane is adjusted further toward the
5   electrode **7** in order that the electrons crossing the path of
the sample gas introduced through the port **12a** will have a
higher energy (about 40 eV). This is accomplished by changing
the switching voltages, as shown in **FIG. 6(b)**, to provide a
positive voltage on electrode **5** in order to continue focusing
10   electrons in parallel paths, as shown in **FIG. 3(b)**, and to
provide a more negative voltage on the electrode **7**. For
extraction of the positive ions, the voltages applied to the
electrodes **5** and **7** are reversed in polarity during the ion
cycle. By using high-voltage, full-floating switching elec-
15   tronics responsive to the signal for switching cycle timing,
as described by the inventors in a paper titled "High-voltage,
full-floating 10-MHz square-wave generator with phase con-
trol," Rev. of Sci. Instr., **60**, 779 (1989), and in a copending
U.S. patent application filed March 31, 1989, Serial No.
20   07/331,160, fast switching of the lens potentials are
achieved.

A fast (50 ns) rise-time high-frequency square-wave
generator is disclosed in that paper and patent application
that is capable of switching between arbitrary voltages of
25   high potential difference using high-current drivers for power
field-effect transistors. Switching signals are provided to
the high-current drivers from a logic network through optoiso-
lators. High-voltage square-wave pulse trains of controllable
phase are produced in the logic network. Other phase-adjust
30   logic networks may, of course, be employed as well as other
drivers for high power field-effect transistors. Square-wave
pulse trains of variable duty cycle are used, and they permit
easy observation of the ion pulses as they arrive synchronous-
ly during the ion on cycle. Typical ion arrival-detection
35   characteristics are shown in the timing diagram of **FIG. 4(a)**

where the waveform **A** represents the timing of the high-voltage square wave applied for ion extraction, and the waveform **B** represents the time-of-flight (TOF) of the ions which is complete after 25 μs. **FIG. 4(b)** illustrates the TOF response

5   for one ion extraction period shown in **FIG. 4(a)**. Note that the ion intensity at the detector of the quadrupole analyzer 20 shown in **FIG. 3(c)** drops off quickly once the signal associated with the "ion on" cycle is initiated. The ion signal burst arrives at the detector approximately 15 μs after the

10   ion extraction voltage is applied as shown in **FIG. 4(b)**. That time delay corresponds to the TOF of the chlorine ions from the reversal region **R** after production from CCl_4.

Extracted ions are focused onto the exit window **W** with a final energy, angular divergence and diameter suitable for

15   the quadrupole mass analyzer **20** shown as a functional block in **FIG. 3(c)**. Detection is achieved in such a mass analyzer by means of a channel-type electron multiplier and pulse amplifiers.

20   Design of the Ionization Region
1. The Electrostatic Mirror

Typical electron filament sources employ a Pierce geometry [J.R. Pierce, J. Appl. Phys. **11**, 548 (1940)] for the efficient electron extraction while maintaining a parallel

25   axially-flowing beam. This is accomplished by the electrostatic potential that the electrode geometry sets up which counteracts space-charge repulsion of the electrons during initial acceleration from the filament. It therefore follows that a reverse-Pierce geometry would facilitate maintaining an

30   axial beam during deceleration by the optical principle of reciprocity. In practice, slight modifications are necessary, which will now be explained.

In one dimension, the Child-Langmuir space-charge law can be rearranged to show that the potential varies as the 4/3

power of the distance x between the cathodic emitter and the
accelerating anode (Wehnelt electrode), viz:

$$V(x) = \left(\frac{9}{4\varepsilon_o\sqrt{2q/m}}\right)^{2/3} J^{2/3}x^{4/3} \qquad (5)$$

where V represents the emitter-accelerator potential, J is the
magnitude of the current density, ε_o is the permittivity of
free space and $q/m = 1.759\times10^{11}$ C kg^{-1} for electrons.

A two-dimensional description in rectangular coordi-
nates if found by conformal transformation where now substitu-
tions are made by orthogonal functions satisfying the
Cauchy-Riemann relations.   It will be found that the V=0
surface originates at the origin (x,y = 0) and will be a
straight line subtending an angle $\theta = 3\pi/8$ to the x-axis. This
represents an electrode placed around the cathode F and typi-
cally held at the same potential.   The anode surface is more
difficult to evaluate analytically, but the numerical trend
leads to a Wehnelt electrode shape that is less conical near
the beam path.   This is the well-known Pierce-electrode geo-
metrical arrangement and is shown in **FIG. 5(a)**. The operation
described is independent of time, hence under time-reversal a
beam parallel to the optical axis will remain paraxial as it
is decelerated in the same electrostatic arrangement.

By numerical simulation a modified geometry was calcu-
lated for the cylindrically-symmetric case which would also
serve as an electrostatic mirror, achieving paraxial flow
during deceleration.   In this case, the reverse-anode would be
more conical than the reverse-Pierce element, as shown in
FIG.5(b). Then, at the reversal point (the position of the
imaginary cathodic filament), the absolute velocity of the
space-charge limited electron beam would be zero, with no
tangential component.

2. Ion Extraction

Ions are formed by electron attachment or DA to the target gas in the electron-reversal region **R**. To prevent a large current of electrons from reaching the window **W** and the mass analyzer, it is desirable to switch off the electrons and wait for electrons to disperse under coulombic repulsion. This time interval should be chosen short enough so that the slower-moving ions migrate only slightly from their point of origin. In practice, the switching-off is accomplished in 50 ns, and the ion extraction voltage (50 ns risetime) is initiated 0.5 - 3 μs later.

In addition, the bulk of ions are inconveniently in the middle of the electron mirror, not in a position conducive to easy extraction. Therefore, an adequately shaped ion extractor electrode, acting under pulsed high potential out of phase by a half cycle to the electron focusing system is employed for efficient ion collection. All electrode shapes have been optimized by computer-assisted numerical simulation of the potential field and the equations of motion, taking into consideration the thermal drift of the ions due to their kinetic energy at onset.

3. The Combined System

Combining the electron reversal and ion extraction geometry is achieved by sharing the middle electrodes **6** as is shown in **FIG. 2**, and in **FIGs. 6(a)** and **(b)**. The two electrodes **6** and **7** form the final mirror field. The electrode **5** forms the initial field of the electrostatic mirror. During the ion extraction cycle, electrode **5** is biased to repel the ions formed between electrodes **5** and **6** while electrode **7** is held at a high potential appropriate for ion extraction. The potential electrode **6** is chosen to provide suitable lens action at the interfaces of electrodes **5** and **6**, and electrodes **6** and **7** improving the efficiency of ion extraction in this region to 100%.

Shown also in **FIG. 2** is the gas inlet annular port **12a** in electrode **6**. Considering only molecular gas flow under an operating vacuum of 10^{-8} torr, the effluent gas forms a narrow "jet" distribution. Its greatest density is thus reasonably

5   confined to the midpoint on the axis between electrodes 5 and **6**, as shown in **FIGs. 3(a)** and **3(c)**.

By adjusting the voltages properly, the reversal point can be moved to the right of the molecular beam's greatest density so as to achieve nonzero electron energy interactions

10   in the collison region. In practice, electron bombardment energies as high as 200 eV have been achieved. This tunable arrangement allows for the production of positive ions, typically achieved at bombarding energies of 50-80 eV. The system then behaves as a conventional residual gas analyzer.

15

Test Results

(a) Experimental Arrangement

The present system accomplished mass analysis using an Extrel quadrupole mass spectrometer which can provide unit

20   mass resolution up to 500 amu. The arrangement of **FIGs. 1a** and **1b** and the quadrupole mass filter were housed in a stainless steel UHV chamber, lined with 1.5 mm thick mu metal to shield external magnetic fields to less than 10 mG over the electrode region from electrodes **3** to **8**, inclusive. The

25   chamber was pumped by a 1500 ℓ/s (air) Edwards oil-diffusion pump with a liquid nitrogen trap. Operating pressures with gas load were between 1.0×10^{-8} and 5.0×10^{-7} torr, with a base pressure of 5.0×10^{-9} torr.

Samples of high purity gases and liquids were obtained

30   from the Matheson Gas Co. and Aldrich Chemical Co. The liquids involved were housed in special pyrex ampules and were subjected to at least five freeze-thaw cycles to remove trapped air. Prior to entering the port **12a** of the system, a precision leak valve was employed to deliver reproducible gas

35   flows to the electron-reversal region. All lines and valves

were wrapped in heating tape and warmed to 350 K to prevent condensation and/or adsorption of the vapors in the apparatus.

The data handling system consisted of a preamplifier wired to the quadrupole's channeltron detector, which delivers signals to a TTL digital circuit producing 5-volt pulses corresponding to counts above a preset threshold. Signal intensity per mass is read on either an Ortec count-rate meter, or on a single-channel scaler. No provision was made for computer control or multichannel scaling analysis.

(b) Sample Runs

In order to demonstrate the operation of the system **FIGs. 7(a-f)** show electron attachment and DA results in CCl_4, SF_6, $CHCl_3$, $1,1,2-C_2Cl_3F_3$ and $c-C_6F_{10}$. These results demonstrate the formation of parent negative ions via virtual states at zero electron energy shown in **FIG. 7(b,f)**; DA fragments via virtual states at zero energy shown in **FIG. 7(a,e)**; DA fragments via real states at nonzero energy corresponding to a reversal point to the right of **R** shown in **FIG. 7(d)** (the $CHCl_3$ resonance lies at 0.37 eV); and parent negative ions via real states at nonzero energy shown in **FIG. 7(c)** (the SF_5^- resonance lies at 0.39 eV). The experiments were also able to resolve clearly the $^{35,37}Cl^-$ isotopes in **FIGs. 7(a,d,e)**. The ratio of peak heights varies with the quadrupole pole bias, and does not necessarily correspond to the natural isotope ratio.

The question naturally arises as to the sensitivity of the ionization system for detection of the molecular targets of **FIG.7(a-f)**. To determine the sensitivity, one of the targets, CCl_4, was chosen and the method of standard additions was used. A mixture of CCl_4 in nitrogen was prepared, and the Cl^- count rate was measured as a function of the concentration C of the mixture.

Mixtures were prepared in an all stainless steel vacuum system capable of being heated to 350 K. Reagent grade CCl_4,

having undergone eight freeze-thaw cycles was mixed with N_2 (99.99% purity) in a concentration ratio C (particle density) = 1 (pure CCl_4) to 5×10^{-7}. The quadrupole mass spectrometer was tuned on mass 35, and the Cl^- signal measured at each C to

5   a statistical accuracy of 3%. Care was taken in the concentration range $10^{-7} < C < 10^{-3}$ to ensure that the mixture was stable; i.e., there was no depletion of the CCl_4 through wall adsorption or chemical reaction. This stability was checked at the lower concentrations by monitoring the Cl^- signal over

10   a period of 1 hour at $C = 1.0 \times 10^{-6}$. The signal was constant at the 5% level.

Results of the standard additions calibration are shown in **FIG. 8.** The errors shown represent the quadrature sum of the statistical counting error and the error in reading the

15   two pressure gauges. The electron current was 2.8×10^{-6} amperes, and the pressure at the gas inlet only was estimated to be in the range 10^{-7} to 10^{-6} torr. One sees in **FIG. 8** a uniform decrease of signal with concentration from 8.4 kHz at $C = 1.0$ to 130 Hz at $C = 5.0 \times 10^{-7}$. It is believed that this lower

20   limit can be extended to the 10^{-8} range in a straightforward fashion, mainly by increasing the duty cycle of the ion extraction by a factor of 16.

Although preferred embodiments of the invention have been described and illustrated herein, it is recognized that

25   modifications, improvements and equivalents may readily occur to those skilled in this art, particularly in improvements on electron current, beam size, collision volume and the like, which are currently being examined. Consequently, it is intended that the claims be interpreted to cover such modifi-

30   cations, improvements and equivalents.

2|
~~24~~

REVERSAL ELECTRON ATTACHMENT
IONIZER FOR DETECTION OF TRACE SPECIES

5   ABSTRACT OF THE DISCLOSURE

An in-line reversal electron, high-current ionizer
capable of focusing a beam of electrons to a reversal region
10   and executing a reversal of said electrons, such that the
electrons possess zero kinetic energy at the point of rever-
sal, may be used to produce both negative and positive ions. A
sample gas is introduced at the point of electron reversal for
low energy electron-(sample gas) molecule attachment with high
15   efficiency. The attachment process produces negative ions
from the sample gas, which includes species present in trace
(minute) amounts. These ions are extracted efficiently and
directed to a mass analyzer where they may be detected and
identified. The generation and detection of positive ions is
20   accomplished in a similar fashion with minimal adjustment to
potentials applied to the apparatus.